A Software for Simulation and Controller Development for High Frequency High Voltage Power Supplies

Prof. Dr. H. Bülent Ertan
Middle East Technical University
Department of Electrical and Electronics Engineering
Ankara-Turkey
Phone : (90) 312 210 23 59 Fax : (90) 312 210 12 61
ertan@metu.edu.tr

Tolga Çamlıkaya   Okan Demirel
Çoşku Kasnakoğlu
Information Technologies and Electronics
Research Institute
Ankara-Turkey

Abstract-*This paper describes a software developed for the simulation of high voltage (up to 125 kV), high frequency power supply for radiology equipment. The main components of the power supply are an AC-DC conversion stage, a high frequency inverter feeding a resonant load. The resonant load is the impedance reflected to the inverter side of the, high voltage, high frequency transformer feeding the X-ray tube. The software has modules for each of the components of the converter mentioned above, which can be modified to accommodate configuration changes. The set of time domain equations for each modules are capable of representing the operation of the related circuits at different states of the switches. Predictor-Modifier-Corrector method is used for solving the resulting set of equations. A control module is incorporated into the software. In the presentation here the control module has a fuzzy controller. The paper first illustrates solution accuracy of the model used. Then the prediction accuracy of the performance of the system is demonstrated.*

Key words : resonant power supply, radiology, software

1. Introduction

A high frequency (typically 15-20 kHz) inverter, supplying a resonant load, formed by the high frequency high voltage transformer parasitic inductance and capacitance and tube impedance powers modern radiology equipment. This is advantageous as the X-ray tube requires a high voltage (up to 125-150 kV) and the inverter DC bus level is typically in the 300-500 V range. Therefore, the transformer turns ratio is very high. This increases the size and cost of the transformer, the gain of the resonant circuit however, reduces the turns ratio and therefore the cost and size.

In radiology the ripple on the cathode voltage of the tube, rise time of the voltage, etc. are very important in determining the quality of the equipment. The control approach therefore, as well as the hardware is extremely important to meet the specifications. This study was initiated to find out whether relatively new intelligent control approaches such as fuzzy control and neural network strategies could be utilized to design a power
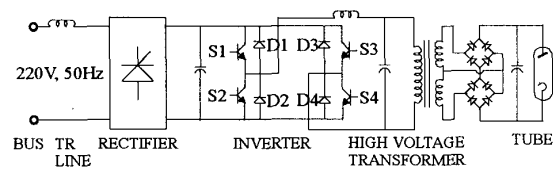

Fig. 1 The circuit of the HV high frequency supply

supply that could achieve the desired quality and also perhaps avoid necessity of a HV side feedback and sense aging of the transformer and also introduce a number of other attractive features.

For simulation of the type of circuits considered in this paper SPICE based software can be used. However, such software is intended more for studying device behavior, and does not allow a study on the controller behavior. MATLAB based modeling of the system is also possible and in this case the controller behavior can also be studied. However, dedicated software is naturally faster and if written appropriately can provide more flexibility.

1.1 The Circuit

The circuit considered in this study is shown in Fig.1. As can be seen from this figure, in the model, impedance of he transmission line to a bus is also considered in the model. This was found essential to consider the effect of this impedance on the system behavior. This may be important as the current demand of the system may be quite high during starting and the grid connection may be weak.

The input side rectifier is a full wave bridge rectifier here. However, other arrangements can be accommodated. This is followed by a filter, which feeds the inverter. The H bridge inverter has IGBT switches and feeds a transformer which raises the inverter output voltage to the levels required by the X-ray tube. The output of the transformer is rectified and filtered and is connected to the X-ray tube which operated at voltage levels reaching 150 kV or so.

The inverter in the circuit is capable of operating in 15-20 kHz region. In this frequency range naturally the size of the transformer is considerably reduced. The actual operating frequency of the inverter depends on the

– 665 –

resonance frequency of the impedance observed at the load terminals of the inverter. In this manner the gain of the resonant circuit helps to reduce the turns ratio of the transformer.

To control the output voltage of the inverter which is supplied from a substantially constant dc voltage source, phase-shift PWM strategy is used. For obtaining the maximum output voltage switches S_1 and S_4 and S_3 and S_4 are simultaneously switched. However, the gating signals of switches S_3 and S_4 are delayed by 180°. The output waveform of the inverter for this condition is shown in Fig 2a. To reduce the output voltage, the gating signals to transistors S_1 and S_2 are shifted by an angle ϕ as show in Fig. 2b with respect to the maximum voltage case where ϕ is zero.
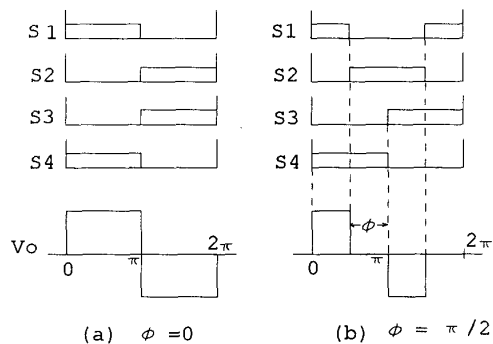

Fig. 2 Switching Sequences for Inverter

2. Mathematical Model

It is essential to have an accurate model (of the system which can represent the its behavior under all operating conditions. In the study here for this purpose, a transformer model referred to the primary (low voltage) side is used. The model consists of a resistance, leakage inductance and stray capacitance of the windings. Naturally, circuit components on the secondary are also referred to the primary in the usual manner. Then, the equivalent circuit of the system becomes as shown in Fig. 3

The configuration (mode) of the circuit above changes according to the state of the switches. Therefore, it is necessary to write down the equations describing the circuit for each mode of operation. In writing the equations the following assumptions are made;
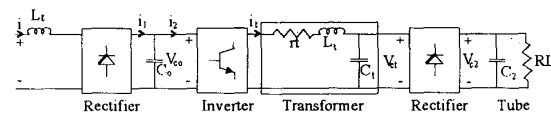

Fig. 3 General model of the power supply

a) Switching devices are ideal, b) Capacitors and inductors are ideal without losses, c) Wiring inductance and resistance are negligibly small.

The state variables of the circuit are chosen as i, V_{co}, i_t, V_{ct} and V_{cz}

2.1 AC/DC Converter Equations

With the labeling convention used in Fig.3 the equations describing the circuit can be written for the three modes of operation possible as follows :

Mode 1 : (C_o is charging an $V_1 \geq 0$)

$$\frac{di}{dt} = \frac{V_1}{L_1} - \frac{V_{co}}{L_1}$$

$$\frac{dV_{co}}{dt} = \frac{i_1}{C_o} - \frac{i_2}{C_o}$$

$$i = i_1$$

Mode 2 : (C_o is charging, $V_1 < 0$)

$$\frac{di}{dt} = \frac{V_1}{L_1} + \frac{V_{co}}{L_1}$$

$$\frac{dV_{co}}{dt} = \frac{i_1}{C_o} - \frac{i_2}{C_o}$$

$$i = -i_1$$

Mode 3 : (C_o is discharging)

$$\frac{dV_{co}}{dt} = -\frac{i_2}{C_o}$$

$$i = 0$$

2.2 DC/DC Converter Equations

In the DC-DC converter part, there are actually twelve operating modes of the system. However, it is enough to analyze the circuit in six modes and use symmetry or the other six. These six modes are shown in Figure 4 and the equations for these modes are as follows with the labeling convention used in Figure 3 :

Mode 1 :

$$\frac{di_t}{dt} = -\frac{r_t}{L_t}i_t - \frac{1}{L_t}V_{ct} + \frac{V_{co}}{L_t}$$

$$\frac{dV_{ct}}{dt} = \frac{1}{C_t}i_t$$

$$\frac{dV_{c2}}{dt} = -\frac{1}{R_L.C_2}V_{c2}$$

Mode 2:

$$\frac{di_t}{dt} = -\frac{r_t}{L_t}i_t - \frac{1}{L_t}V_{ct} + \frac{V_{co}}{L_t}$$

$$\frac{dV_{ct}}{dt} = \frac{1}{C_t + C_2}i_t - \frac{1}{R_L.(C_t + C_2)}V_{ct}$$
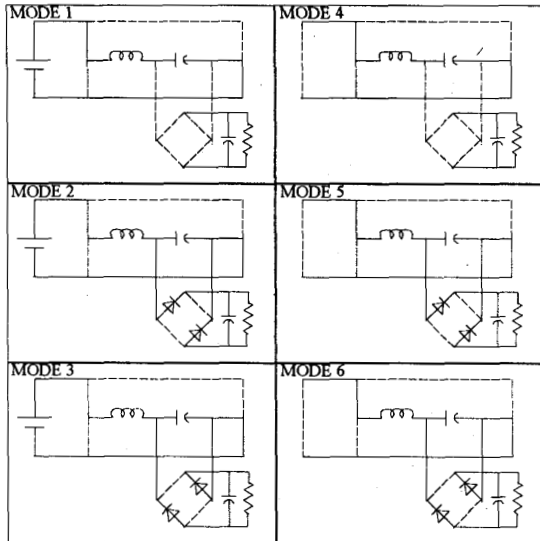
$$V_{c2} = V_{ct}$$

Fig. 4 Modes of operation of the inverter

Mode 3:

$$\frac{di_t}{dt} = -\frac{r_t}{L_t}i_t - \frac{1}{L_t}V_{ct} + \frac{V_{co}}{L_t}$$

$$\frac{dV_{ct}}{dt} = \frac{1}{C_t + C_2}i_t - \frac{1}{R_L.(C_t + C_2)}V_{ct}$$

$$V_{c2} = -V_{ct}$$

Mode 4:

$$\frac{di_t}{dt} = -\frac{r_t}{L_t}i_t - \frac{1}{L_t}V_{ct}$$

$$\frac{dV_{ct}}{dt} = \frac{1}{C_t}i_t$$

$$\frac{dV_{c2}}{dt} = -\frac{1}{R_L.C_2}V_{c2}$$

Mode 5:

$$\frac{di_t}{dt} = -\frac{r_t}{L_t}i_t - \frac{1}{L_t}V_{ct}$$

$$\frac{dV_{ct}}{dt} = \frac{1}{C_t + C_2}i_t - \frac{1}{R_L.(C_t + C_2)}V_{ct}$$

$$V_{c2} = V_{ct}$$

Mode 6:

$$\frac{di_t}{dt} = -\frac{r_t}{L_t}i_t - \frac{1}{L_t}V_{ct}$$

$$\frac{dV_{ct}}{dt} = \frac{1}{C_t + C_2}i_t - \frac{1}{R_L.(C_t + C_2)}V_{ct}$$

$$V_{c2} = -V_{ct}$$

3. Numerical Solution

The system can be defined in terms of differential equations given above and a total number of five state variables: i, V_{co}, i_t, V_{ct}, V_{c2}. Analyzing the circuit requires solving these equations and obtaining the functions $i(t)$, $V_{co}(t)$, $i_t(t)$, $V_{ct}(t)$, $V_{c2}(t)$.

The exact analytical solutions of these types of equations rarely exist. Even if there is one, it is very hard and time-consuming task to go for it. Furthermore, the function obtained at the end might be too complicated to be of any use. For this reasons in this study numerical techniques are used for the solution. The method applied in the computer simulation of the system is known as the Predictor-Modifier-Corrector method.

Using a numerical solution method for the system analysis requires iteration, starting from the initial values of the variables, and continuing until the end of the solution period is reached. We shall denote the equation to be solved as:

$$\frac{dy}{dt} = f(i, V_{co}, i_t, V_{ct}, V_{c2}, t)$$

where y is the state variable of interest, and f is a function of all 5 state variables and time. The following notation will also be assumed:

t : Current time
Δt : Time step
y_j : Result obtained for current time
y_{j-k} : Result obtained for the kth step before current time
y_{j+1} : Approximate result for the step following first iter.
f_j : f evaluated for current time
f_{j-k} : f evaluated with the values obtained k steps before.

The equations used for the computer simulation are:

Predictor :

$$y_{j+1}^{(0)} = y_j + \Delta t(\frac{55}{24}f_j - \frac{59}{24}f_{j-1} + \frac{37}{24}f_{j-2} - \frac{9}{24}f_{j-3})$$

(Fourth order Adams-Bashforth type formula)

Modifier :

$$\bar{y}_{j+1}^{(0)} = y_{j+1}^{(0)} - \frac{251}{270}(y_j - y_j^{(0)})$$

Corrector :

$$y_{j+1}^{(t+1)} = y_j + \Delta t(\frac{9}{24}f_{j+1}^t + \frac{19}{24}f_j - \frac{5}{24}f_{j-1} + \frac{1}{24}f_{j-2})$$

(Fourth order Adams-Moulton type formula)

These equations depend on the previous values of y, which means that they are not *self-starting* and very first values of the solution process should be calculated by other methods to initiate the simulation. For this purpose, the solution is started with the **Runge-Kutta** type equations. Although this approach is less efficient and less accurate than the above ones, this does not produce a major change in the program speed, since they will only be performed for a small and constant number of iterations.

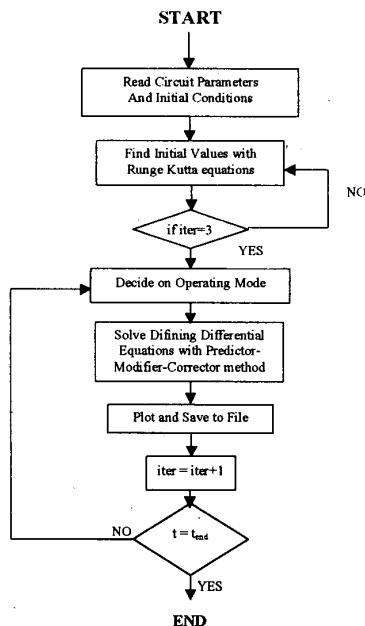The major blocks of the simulation software are shown in Fig. 5

START

Fig. 5 Flowchart of the software

4. Fuzzy Controller Module

The purpose of the controller in this problem is to assure that the voltage on the tube reaches the set value in the shortest possible time and remains at that value within a few percent of the desired voltage. Fig. 11 shows the (referred to primers) voltage on the tube if the phase shift angle is fixed at a certain value. Note that the rise time of the tube voltage is about 90 msec and there is a 100 Hz (6 %)) ripple on the tube voltage. Furthermore a high frequency, smaller magnitude (2 %) ripple is observable on the tube voltage. The rise time is unacceptably high and must be reduced. The 100 Hz

ripple must be eliminated also. However, there is little that can be done to eliminate the high frequency ripple, stemming from the operation of the inverter, other than filtering it.

Due to the highly nonlinear circuit of the system fuzzy control (FC) is found to be most suitable for the application here.

In the approach here, change in phase-shift angle, deltaPhi, of the inverter is the calculated fuzzy output. The new control angle therefore is;

phi$_{new}$ = phi$_{old}$ + deltaPhi

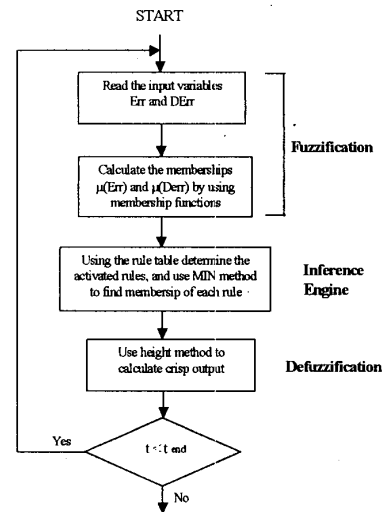Flow chart of the program is given in Fig. 6.

Fig. 6 Flowchart of the Fuzzy controller

Crisp inputs to the fuzzy controller are error on the tube voltage and the derivative of the error, which are represented by "Err(k)" and "Derr(k)" respectively. These values are calculated as follows:

Err(k) = V(k) - Vset
DErr(k) = Err(k) - Err(k-1)

Where

V(k) = Output voltage signal
V$_{set}$ = Preset reference signal

After the calculation of the crisp input variables, fuzzification is performed by establishing the variation intervals of the variables to be controlled and defining a number of membership functions inside such intervals. The overall performance of the system is affected by the shapes and number of the membership functions that are chosen according to the experience of expert people about the process. The membership functions can be in triangular, trapezoidal or exponential shapes. Membership functions of Err and DErr are given in Fig. 7. According to these membership functions, two fuzzy

– 668 –

variables are activated for each input. At this point fuzzy variables of our system is introduced as follows:
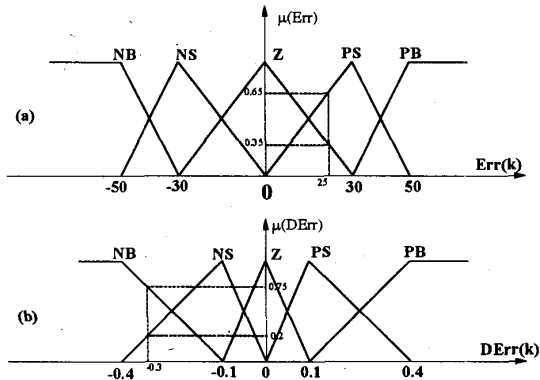

Fig. 7 Membership Functions for
(a) Error (b) Derivative Error

NB : Negative Big
NS : Negative Small
Z : Zero
PS : Positive Small
PB : Positive Big

Activated rules by the input fuzzy variables are determined by using the *rule base*. Rule base determines the behaviour of the controller, and this is why the most important feature of the fuzzy logic controller is to generate the fuzzy control rules in an appropriate manner. Rule base of the FC is given in Table 2.

Table 1. Rule Base Table

DErr Err	NB	NS	Z	PS	PB
NB	NB	NB	NB	NS	Z
NS	NB	NS	NS	Z	PB
Z	NB	NS	Z	PS	PB
PS	NS	Z	PS	PS	PB
PB	Z	PS	PB	PB	PB

Between each rule, union operation applied if the same rule is activated. At this point, function of the inference engine is completed by the determination of rules and the membership of each rule.

In the application here the height method is used for defuzzfication since it is both a very simple and very quick method. Membership function of DeltaPhi is given

in Fig. 8 and driven rules are marked on them with the individual membership values.
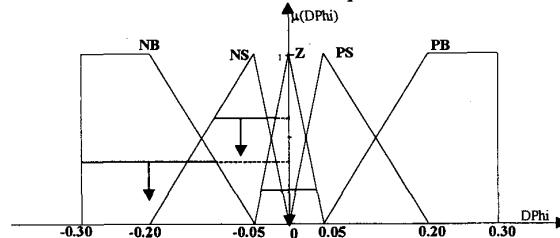

Fig. 8 Membership Function of DeltaPhi

5. The Software

The main user interface window of the simulation software (NuXs) developed is shown in Fig. 9. The software allows user to modify all the circuit parameters and assign commands to the software to study a certain operating conditions. There are thee main user interface windows of the program.

1. Main window (Fig. 9)
2. Parameter window (Fig. 10)
3. Graphics window (Fig. 11)
4. Fuzzy control window

The software has a fuzzy controller which is described in Section 4, as well as a neural net type control which is not described here. The type of control can be chosen by checking the appropriate box, on the main window. Parameter window is self-explanatory. The graphics window allows user to plot the desired variable. While the FC window permits changing the rule base table and membership functions.
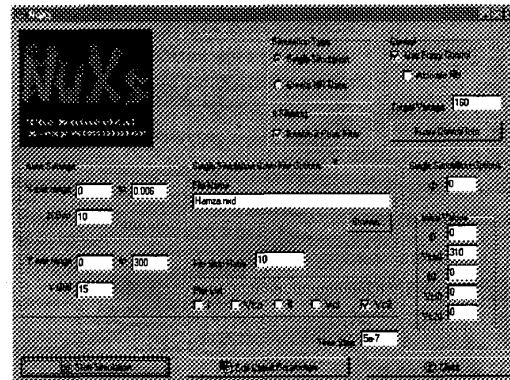

Fig. 9 NuXs Main Window

– 669 –

6. Verification of the Software Accuracy and Conclusions

To verify the accuracy of the developed software initially PSPICE simulations were used. Fig. 11 b displays the Spice simulation result with $V_{co}=0$ and $\emptyset=0$. Comparison of this figure with Fig. 11 a clearly displays that the accuracy of NuXs simulation is very good. Later the software proved itself to be very useful for tuning the fuzzy control parameters. Finalizing the shape of the membership functions or deciding on the rule base table would have otherwise been a dreadful task.

The control system developed using NuXs is later implemented on a TMS320 signal processor, and tested. Fig. 12 shows an experimental result where the tube voltage is shown (referred to primary). This test is performed with the DC link capacitor initially charged to rated value and the controller in operation. It can be observed from the figure that the rise time of the tube voltage is reduced to 0.2 msec and the 100 Hz ripple at the output is totally removed.

In conclusion it can be safely said that a very versatile tool is obtained by developing NuXs, which can be used to study the effect of circuit parameters or to test various control algorithms. Alternatively, the software can be used to tune the controller parameters saving valuable development time.
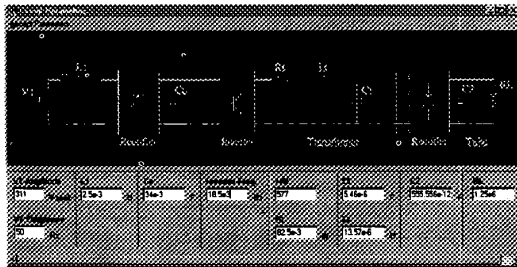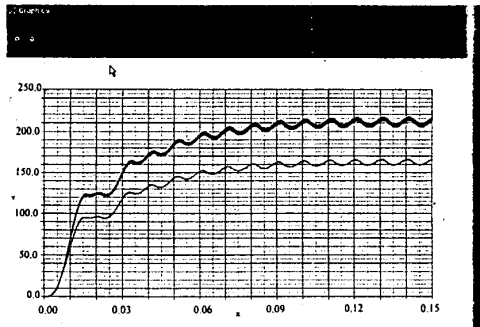
Fig. 10 NuXs Parameter Window

Fig. 11 a) NuXs DC link and referred tube voltage
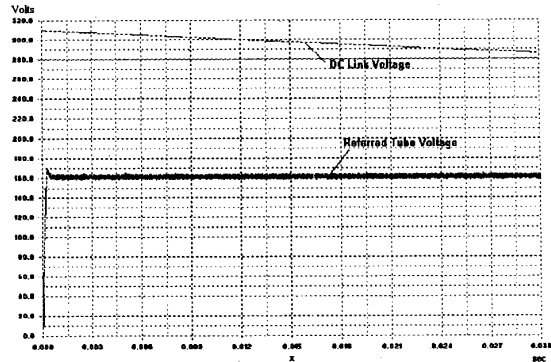$V_{co}=0$ and $\phi=0$ with no control

Fig. 12 Measured DC link voltage (dashed line) and tube voltage (referred)

References

[1]   H. Hino, "High-frequency Parallel Resonant Converter For X-ray Generator Utilizing Parasitic Circuit Constants of High Voltage Transformer and Cables" INTELEC. 89, Eleventh International Telecommunications Energy Conference. Conference Proceeding, Italy, 15-18 October 1989.

[2]   H. Hino, "Digitally Controlled Resonant Converter for X-ray Generator Utilizing Parasitic Circuit Constants of High Voltage Transformer and Cables" EPE89, 3rd European Conference on Power Electronics and Applications, Aachen, West Germany, 9-12 October 1989.

[3]   R. L. Steigerwald, "High-Frequency Resonant Transistor DC-DC Converters", IEEE Trans. on Industrial Electronics, Vol. IE-31, No.2, May 1984.

[4]   I. Eskandarzadeh, "Design and Control of a Phase-Shift PWM Resonant Converter for an X-Ray Generator", PhD Thesis at METU, December 1996.

[5]   T. Camlikaya, "Fuzzy Control of Resonant Inverter Circuit for X-ray Power Supply", MS Thesis, METU, January 1999.

[6]   O. Demirel, "Design And Optimization of High Frequency High Voltage Transformer for Basic Radiology Unit", MS Thesis, Hacettepe University, 1999.
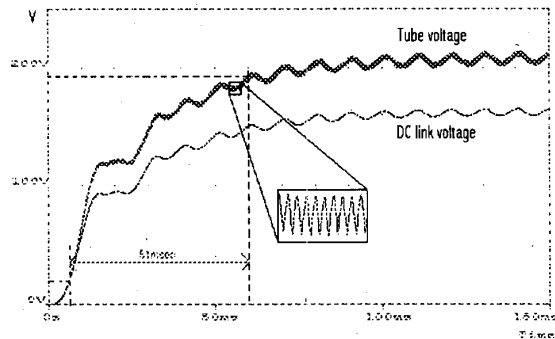
Fig. 11 b) SPICE DC link and referred tube voltage
$V_{co}=0$ and $\phi=0$ with no control